Multiple W_L production from inelastic $W_L W_L$ scattering at $\sqrt{\hat{s}} \gg M_H$

D. A. Morris[*] and R. D. Peccei[†]

Department of Physics, University of California at Los Angeles, Los Angeles, California 90024-1547

R. Rosenfeld[‡]

Department of Physics, Northeastern University, Boston, Massachusetts 02115

(Received 30 November 1992)

We explore the inelastic production of multiple longitudinal weak bosons as a manifestation of a strongly interacting symmetry-breaking sector. By analogy with QCD, final states with large multiplicities are expected to occur not far above the energy scale of the lowest resonances of the underlying strong theory. We consider the feasibility of observing such phenomena in the environment of a very-high-energy hadron collider.

PACS number(s): 13.85.Hd, 11.15.Ex, 12.15.Cc, 14.80.Er

I. INTRODUCTION

One of the most interesting open questions in the minimal standard model (MSM) asks if the breakdown of $SU(2)_L \times U(1)_Y$ is caused by a weakly coupled or strongly coupled theory. The MSM, with a Higgs potential

$$V = \lambda \left(\Phi^\dagger \Phi - \frac{v^2}{2} \right)^2, \tag{1}$$

is prototypical of the first option, at least if $\lambda \ll 1$. Models where the $SU(2)_L \times U(1)_Y$ breakdown is due to fermionic condensates (e.g., $\langle \bar{T}T \rangle$) of some underlying theory nicely typify the other possibility [1], since condensate formation is symptomatic of strong coupling. These two alternatives lead to quite distinct predictions for the scattering amplitudes of longitudinal weak vector bosons $W_L \sim \{W_L^\pm, Z_L\}$. As is well known, through the equivalence theorem of Cornwall, Levin, and Tiktopoulos [2, 3], high-energy $W_L W_L$ scattering is directly related to scattering of the corresponding Goldstone bosons (denoted by $w \sim \{w^\pm, z\}$) ensuing from the symmetry breakdown. If the symmetry-breaking sector is characterized by weak coupling, the scattering among the W_L will be weak. If, on the other hand, there are strong interactions in the symmetry-breaking sector, these will be directly seen in $W_L W_L$ scattering.

This distinction between strong and weak coupling in the symmetry-breaking sector will only be apparent at high energies, since at threshold the physics is the same. Let us momentarily focus on the minimal Higgs model and rewrite the complex field Φ in terms of the triplet of Goldstone boson fields $w^\pm$, z and the physical Higgs field H:

$$\Phi = \begin{pmatrix} \dfrac{v + H + iz}{\sqrt{2}} \\ iw^- \end{pmatrix}. \tag{2}$$

A simple calculation then leads to the following amplitude for the scattering process $w^+ w^- \to zz$:

$$A(w^+ w^- \to zz) = -2\lambda \left[1 + \frac{2\lambda v^2}{s - 2\lambda v^2} \right], \tag{3}$$

where $\sqrt{s}$ is the $w^+ w^-$ center-of-momentum system (cms) energy. Analogous expressions are easily deduced for other channels. At threshold, $s \ll M_H^2 = 2\lambda v^2$, Eq. (3) reduces to a simple expression, which is *independent* of λ:

$$A(w^+ w^- \to zz) \longrightarrow \frac{s}{v^2}, \tag{4}$$

reflecting that the dynamics at that point is solely determined by the coset space of the breakdown — here $O(4)/O(3) \sim [SU(2)_L \times SU(2)_R]/SU(2)_V$. If the $SU(2)_L \times U(1)_Y$ breakdown is due to some strongly coupled theory governed by the same global symmetry pattern as that of the Higgs model, then here also $A(w^+ w^- \to zz)$ at threshold would be given by Eq. (4).

Above the threshold region, however, there are real distinctions between the scattering amplitudes for, say, $w^+ w^- \to zz$ predicted by the Higgs theory and that predicted by some model of dynamical symmetry breakdown. The amplitude of Eq. (3) for the Higgs case, when plotted as a function of s, displays only one remarkable feature—a resonance pole in the $J = 0$ channel at the Higgs-boson mass M_H. For $s \gg M_H^2$ this amplitude goes to a constant

$$A(w^+ w^- \to zz) \to -2\lambda, \tag{5}$$

which for $\lambda \ll 1$ gives weak scattering.

For the case of dynamical symmetry breakdown, in complete analogy with what happens in QCD for $\pi\pi$ scattering, one expects significantly different behavior. First of all, the scattering amplitude should contain resonances

in other partial waves besides $J = 0$:

$$A(w^+ w^- \to zz) = 32\pi \sum_J (2J+1) P_J(\cos\theta) a_J(s). \qquad (6)$$

Second, at energies slightly above those where the first resonance forms, one would also expect a rapid opening up of inelastic channels. Because of this, the partial waves $a_J(s)$ will not have unit strength:

$$a_J(s) = \frac{1}{2i}\left[\eta_J(s)e^{2i\delta_J(s)} - 1\right], \quad \eta_J(s) < 1. \qquad (7)$$

The search for strongly interacting effects in *elastic* $W_L W_L$ scattering at the CERN Large Hadron Collider (LHC) and the Superconducting Super Collider (SSC) has been a subject of intense interest in recent years, resulting in literally hundreds of papers [4]. On the other hand, *inelastic* $W_L W_L$ scattering, after a pioneering paper by Chanowitz and Gaillard [5], has hardly been investigated. (For recent speculations on the existence of inelastic scattering involving additional Goldstone bosons see Ref. [6].) This dichotomy in treatment is not difficult to understand. Both the LHC and SSC are machines that are barely above threshold as far as $W_L W_L$ scattering goes. Thus, one is already pushed relatively hard to dig out a signal for resonance formation in the $W_L W_L$ channel, and it is essentially hopeless to see any effects of the opening up of inelastic channels. However, for a machine of even higher energy, like the proposed European Long Intersecting Storage Accelerator (Eloisatron) operating at $\sqrt{s} = 200$ TeV these signals should become more apparent. In some ways multi-W_L production, when it is prolific, may perhaps be a simpler signal to detect, and it will provide an equally distinct telltale sign of having strong dynamics in the $W_L W_L$ channel. The purpose of this paper is to characterize and quantify as best as one can this second aspect of having strong dynamics in the symmetry-breaking sector.

Because, as of yet, no one has a clear idea of the detailed dynamics of a strongly coupled symmetry-breaking sector, we will have to make certain assumptions regarding the threshold for copious multiparticle production and the nature of the signal beyond that threshold. We will be guided in making these assumptions by, among other things, the pattern of cross sections and multiplicity distributions that are observed in hadronic interactions. We will, however, make some further simplifying assumptions whenever they appear warranted. This is a sensible approach to take, since there is no reason why an underlying strong theory, which produces the breakdown of $SU(2)_L \times U(1)_Y$, should blindly copy QCD. Furthermore, we also cannot pretend that the details we obtain will be trustworthy. Nevertheless, we feel that the broad features that emerge from our study, despite our simplifying assumptions, should turn out to be generally correct.

The paper is organized as follows. In Sec. II we review the connection between pions (denoted by $\pi \sim \{\pi^\pm, \pi^0\}$) and the Goldstone bosons w associated with weak symmetry breaking. Pursuing the notion of strong dynamics in the weak symmetry-breaking sector, we use our inferred knowledge of strong inelastic $\pi\pi$ scattering as a template and scale it up from GeV energies to TeV en-

ergies to describe strong inelastic ww scattering. In Sec. III we incorporate the assumed strong ww dynamics into calculations appropriate for proton-proton scattering. In Sec. IV we present a rough comparison of multi-w signatures of strong inelastic ww scattering to multigauge-boson backgrounds expected in the MSM. In Sec. V we summarize our results and conclude.

II. SCALING FROM GeV TO TeV

The reason for drawing an analogy between the Goldstone bosons $w^\pm, z$ and pions originates from the observation [7, 3] that the symmetry-breaking Lagrangian of the MSM is that of a $SU(2)_L \times SU(2)_R$ chirally symmetric linear σ model (LSM) [8] — the same type of model as that successfully describing low-energy $\pi\pi$ scattering ($\sqrt{s_{\pi\pi}} \lesssim 1$ GeV) [9]. The correspondence between the two theories may be expressed by associating

$$w \to \pi, \qquad (8)$$

$$H \to \sigma, \qquad (9)$$

$$v \simeq 246 \text{ GeV} \to f_\pi \simeq 93 \text{ MeV}. \qquad (10)$$

Thus, at least on a formal level, LSM predictions for low-energy $\pi\pi$ scattering may be related to MSM predictions for ww scattering at a cms energy $\sqrt{s_{ww}}$ by equating [3, 10]

$$\sqrt{s_{ww}} = \frac{v}{f_\pi}\sqrt{s_{\pi\pi}}. \qquad (11)$$

In order to demonstrate the possible consequences of strong inelastic ww scattering we will, for definiteness, interpret Eq. (11) literally and use it to map inelastic $\pi\pi$ physics (inferred from known hadron phenomenology) to hypothetically strong ww interactions [11]. We cannot overemphasize the extent to which this assumption is largely unsubstantiated — it is made in the spirit of simplicity rather than absolute correctness. In effect, we will have elevated the status of Eq. (11) from being a relationship between the limiting cases of two *models* (the LSM of low-energy pion physics and the Higgs sector of the MSM) to assuming it is a relationship between the *actual physics* of pions and the *actual physics* of the Goldstone bosons w. Strictly speaking, the LSM description of elastic $\pi\pi$ physics [and, by association, Eq. (11)] is only valid for $\sqrt{s_{\pi\pi}} \lesssim 1$ GeV, whereas we are interested in inelastic $\pi\pi$ physics typified by $\sqrt{s_{\pi\pi}} \gtrsim 1$ GeV. With respect to the Goldstone bosons w, the assumed literal equivalence to π physics implies that if the MSM Higgs sector is only an effective theory of some underlying theory such as technicolor, then we have ignored the possibility of their being additional Goldstone bosons in the spectrum [6]. If we were to go beyond the MSM Higgs sector and assume, for example, a N_{TC} technicolor model, we should consider replacing Eq. (11) with [12]

$$\sqrt{s_{ww}} = \frac{v}{f_\pi}\sqrt{\frac{3}{N_{TC}}}\sqrt{s_{\pi\pi}}. \qquad (12)$$

Again, in the interest of simplicity, we shall ignore this embellishment and others [13] except to note that in some

instances they suggest lower (and hence more accessible) energy scales for ww physics.

To the extent that we scale energies according to a factor of v/f_π and use $\pi\pi$ physics as a guideline, we now turn to parametrizing multi-w production with motivation from hadronic phenomenology. A casual inspection of data [14] for $\sigma_{\text{total}}^{pp}(\sqrt{s})$, $\sigma_{\text{total}}^{\pi p}(\sqrt{s})$, etc., reveals many salient features of hadron scattering. The region $\sqrt{s} \lesssim 1 - 2$ GeV is typically dominated by resonance formation characterized by large fluctuations in the cross section. For $\sqrt{s} \gtrsim 1 - 2$ GeV *elastic* cross sections decrease rapidly, while total cross sections remain almost constant apart from an eventual slow growth, which does not interest us here. This behavior, corresponding to the sudden onset of multiparticle production, originates from the on-shell production and decay of many low-lying resonances. Essentially all of the produced particles are pions.

Though direct $\pi\pi$ scattering is not experimentally feasible, it is reasonable to expect that $\sigma_{\text{total}}^{\pi\pi}(\sqrt{s})$ also exhibits the generic features of baryon-baryon and meson-baryon total cross sections. In fact, since for fixed $\sqrt{s}$ a smaller fraction of the available energy is invested in the rest masses of the initial pions (compared to scattering involving baryons), one expects multipion production to set in at even lower cms energies (i.e., with $\sqrt{s}$ closer to 1 GeV than 2 GeV). Scaling this up by v/f_π implies a corresponding onset of multi-w production for ww cms energies above a threshold of $\sqrt{\hat{s}_0} \simeq 2.5-5$ TeV. (The notation anticipates our use of $\sqrt{\hat{s}_0}$ as a subprocess threshold in proton-proton scattering.) In reality, the multi-w threshold would be determined by the physics of the low-lying resonances of the strongly interacting Higgs sector. Hence, if no resonances in $W_L W_L$ scattering are observed at the LHC or SSC, then the corresponding scale of inelastic multi-w production is pushed up (and possibly out of reach of even the Eloisatron). In calculations we will use $\sqrt{\hat{s}_0} = 5$ TeV. In Sec. V we briefly discuss the possible, though perhaps less plausible, scenario of a $\sqrt{\hat{s}_0} = 1$ TeV threshold accessible to the SSC.

Treating $w^\pm, z$ on the same basis, we parametrize the multi-w production cross section at a ww subprocess cms

energy $\sqrt{\hat{s}}$ by

$$\hat{\sigma}_{\text{multi-}w}^{ww} = \hat{\sigma}_0 \Theta(\hat{s} - \hat{s}_0). \tag{13}$$

The θ function restricts our attention to inelastic reactions and, in analogy with hadronic physics, reflects the near constancy of the total cross section above the inelastic threshold. We can motivate a choice for $\hat{\sigma}_0$ in several ways. On purely dimensional grounds, a constant total cross section of $\hat{\sigma}_0 \simeq O(1/v^2) = 6$ nb for strongly interacting Goldstone bosons is a reasonable guess. A similar estimate follows from scaling up $\sigma_{\text{total}}^{\pi\pi}$ which, using the quark model additivity assumption [15], is obtained from

$$\sigma_{\text{total}}^{\pi\pi} = \frac{\left(\sigma_{\text{total}}^{\pi p}\right)^2}{\sigma_{\text{total}}^{pp}} \simeq \frac{(25 \text{ mb})^2}{40 \text{ mb}} \simeq 16 \text{ mb}, \tag{14}$$

where we have used data [14] for $\sigma_{\text{total}}^{\pi p}$ and $\sigma_{\text{total}}^{pp}$. Scaling up this value of $\sigma_{\text{total}}^{\pi\pi}$ by $(f_\pi/v)^2$ gives $\hat{\sigma}_0 \simeq 2$ nb. To be more conservative, we will use $\hat{\sigma}_0 = 1$ nb for our subsequent numerical investigations.

We can estimate the multiplicities of Goldstone bosons in inelastic ww interactions by relating them to pion multiplicities in $\pi\pi$ interactions. However, faced once more with an absence of relevant $\pi\pi$ data, we must proceed indirectly. We first connect the average charged pion multiplicity in $\pi\pi$ interactions to the average charged particle multiplicity (essentially composed of $\pi^\pm$) measured in e^+e^- annihilation. A simple ansatz, motivated by studies that relate mulitiplicity data from pp collisions to multiplicity data from e^+e^- annihilation [16], is to assume that the average charged pion multiplicity for $\pi\pi$ interactions at cms energy $\sqrt{s_{\pi\pi}}$ is given by the average charge multiplicity in e^+e^- annihilation at cms energy $\simeq \sqrt{s_{\pi\pi}}/2$. The factor of $1/2$ attempts to compensate for the circumstance that not all of the energy $\sqrt{s_{\pi\pi}}$ is available for particle production.

As a second step, we connect the average $\pi^\pm$ multiplicities in $\pi\pi$ interactions to $w^\pm$ multiplicities in ww interactions by using Eq. (11). For ww interactions at a subprocess cms energy $\sqrt{\hat{s}}$ we use the following parametrization for the multiplicity of charged Goldstone bosons ($\langle n_w \rangle = \langle n_{w+} + n_{w-} \rangle$),

$$\langle n_w \rangle = \begin{cases} 3.32 - 0.408 \ln\left(\dfrac{\hat{s}_{\text{eff}}}{1 \text{ GeV}^2}\right) + 0.263 \ln^2\left(\dfrac{\hat{s}_{\text{eff}}}{1 \text{ GeV}^2}\right) & \text{if } \sqrt{\hat{s}_{\text{eff}}} > 1.5 \text{ GeV}, \\[2mm] 3.2 & \text{if } \sqrt{\hat{s}_{\text{eff}}} \leq 1.5 \text{ GeV}, \end{cases} \tag{15}$$

where

$$\sqrt{\hat{s}_{\text{eff}}} = \frac{1}{2}\frac{f_\pi}{v}\sqrt{\hat{s}}. \tag{16}$$

The right-hand side of Eq. (15) for $\sqrt{\hat{s}_{\text{eff}}} > 1.5$ GeV is a parametrization of data for the average charge multiplicity in e^+e^- annihilation [17]. Since the parametrization of Ref. [17] is not intended to be used below 1.5 GeV (and is slightly pathologic in that region), we take the average charge multiplicity to be constant for $\sqrt{\hat{s}_{\text{eff}}} < 1.5$ GeV. As it turns out, we will only make use of Eq. (15) in the limited region 0.9 GeV $\lesssim \sqrt{\hat{s}_{\text{eff}}} \lesssim 2$ GeV; hence the pre-

cise details of the parametrization are largely irrelevant. Furthermore, because $\langle n_w \rangle$ is a slowly varying function of $\hat{s}_{\text{eff}}$ in the region of interest, the factor $1/2$ in Eq. (16) is not of major significance — especially considering the more speculative nature of the factor f_π/v. Nevertheless we include the factor of $1/2$ for completeness.

For ww subprocess cms energies $\sqrt{\hat{s}} \gtrsim 5$ TeV, Eq. (15) gives $\langle n_w \rangle \simeq 3 - 4$ suggesting that the distribution of n_w about the average should be well described by a Poisson distribution. Hence, if we assume

$$\langle n_z \rangle = \frac{\langle n_w \rangle}{2} \tag{17}$$

(which is well motivated from hadronic physics), then the probability of obtaining n_w charged Goldstone bosons and n_z neutral Goldstone bosons becomes

$$P(n_w, n_z, \sqrt{\hat{s}}) = \frac{e^{-\langle n_w \rangle} \langle n_w \rangle^{n_w}}{n_w!} \frac{e^{-\langle n_z \rangle} \langle n_z \rangle^{n_z}}{n_z!}. \quad (18)$$

We will incorporate Eqs. (15)–(18) into our quantitative analysis. Strictly speaking Eq. (18) cannot be correct for $n_w + n_z = 0$ or 1 because of energy-momentum conservation. Since our interest will be in high multiplicity states, ignoring this inconsistency actually leads to more conservative results (i.e., it will lead to slightly smaller probabilities for high-multiplicity final states).

III. pp CROSS SECTIONS

Consider an inelastic $W_L W_L$ subprocess above a threshold $\sqrt{\hat{s}_0} = 5$ TeV in the environment of a proton-proton (pp) collider. In the cms of the hard subprocess each initial W_L has an energy E_{W_L} such that

$$\frac{E_{W_L}}{M_W} = \frac{\sqrt{\hat{s}}}{2M_W} \gtrsim 30. \quad (19)$$

By the equivalence theorem [2, 3] we are then quite justified in replacing the longitudinal gauge bosons $W_L^{\pm}, Z_L$ with the corresponding Goldstone bosons $w^{\pm}, z$. With this equivalence in mind we subsequently phrase many
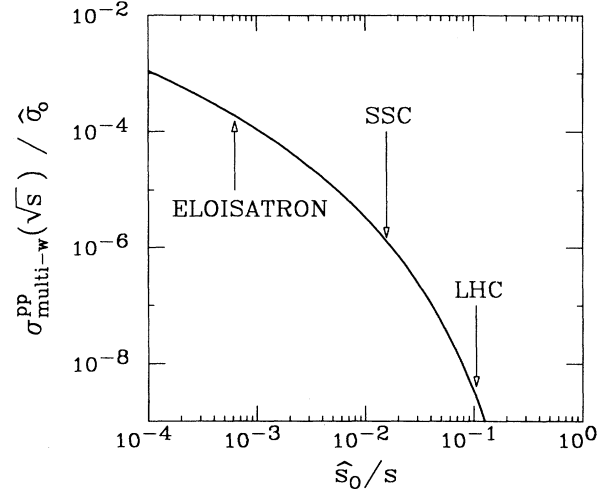

FIG. 1. Proton-proton cross section at center of mass energy $\sqrt{s}$ for subprocess cross section $\hat{\sigma}(ww \to X) = \hat{\sigma}_0 \Theta(\hat{s} - \hat{s}_0)$. Arrows indicate situations relevant to the LHC ($\sqrt{s} = 15.4$ TeV), SSC ($\sqrt{s} = 40$ TeV), and Eloisatron ($\sqrt{s} = 200$ TeV) for an assumed threshold of $\sqrt{\hat{s}_0} = 5$ TeV.

of our results directly in terms of Goldstone bosons.

Let $\sigma_{\text{multi}-w}^{pp}$ denote the pp cross section for multi-w production. The effective vector boson approximation [18] and the parametrization of Eq. (13) give

$$\sigma_{\text{multi}-w}^{pp}(\sqrt{s}) = \sum_{w_i w_j} \int dx_1 \, dx_2 \, f_{w_i}(x_1) f_{w_j}(x_2) \hat{\sigma}_0 \Theta(x_1 x_2 s - \hat{s}_0). \quad (20)$$

The double sum extends over $w_i \sim \{w^{\pm}, z\}$ where $f_{w_i}(x)$ is the distribution function of w_i carrying a fraction x of the original proton momentum.

Specifically,

$$f_{w_i}(x) = \sum_k \int_x^1 \frac{dy}{y} f_k(y) P_{w_i/k}\left(\frac{x}{y}\right), \quad (21)$$

where $f_k(y)$ is the distribution function for quarks (or antiquarks) of species k inside a proton. The splitting function $P_{w_i/k}(x)$ is the probability that a Goldstone boson w_i (or, more appropriately, the associated longitudinal gauge boson) carries away a momentum fraction x from a parent quark of species k. Since we are interested in ww subprocess energies $\sqrt{\hat{s}} \gg M_W$ we are justified in using the leading logarithmic form of the effective vector boson approximation for the splitting functions found in the literature [18]. In our calculations we employ the Morfin-Tung SL-fit leading order distribution functions $f_k(y)$ from Ref. [19] evaluated at $Q^2 = M_W^2$ (which is the scale implied by the emission of an on-mass-shell longitudinal boson).

For later convenience we rewrite Eq. (20) in the form

$$\sigma_{\text{multi}-w}^{pp}(\sqrt{s}) = \int_{\hat{s}_0/s}^1 d\tau \, \mathcal{L}(\tau) \, \hat{\sigma}_0, \quad (22)$$

where $\mathcal{L}(\tau)$ is the ww luminosity function

$$\mathcal{L}(\tau) = \sum_{ij} \int_\tau^1 \frac{dx_1}{x_1} f_{w_i}(x_1) f_{w_j}\left(\frac{\tau}{x_1}\right). \quad (23)$$

Figure 1 plots $\sigma_{\text{multi}-w}^{pp}/\hat{\sigma}_0$ as a function of $\hat{s}_0/s$. With $\sqrt{\hat{s}_0} = 5$ TeV, $\hat{\sigma}_0 = 1$ nb, the Eloisatron ($\sqrt{s} = 200$ TeV) gives $\sigma_{\text{multi}-w}^{pp} \simeq 190$ fb. For purposes of comparison, a machine luminosity of 10^{33} cm^{-2} s^{-1} over a nominal 10^7 s year gives an integrated luminosity of 10 fb^{-1} — corresponding to 1900 events (before considering branching fractions, detector acceptance, efficiency, etc.).

The Goldstone boson multiplicity distribution for pp collisions may be expressed in terms of the ww luminosity of Eq. (23) and the subprocess multiplicity of Eq. (18):

$$\tilde{P}(n_w, n_w, \sqrt{s}) = \frac{\int_{\hat{s}_0/s}^1 d\tau \, \mathcal{L}(\tau) P(n_w, n_z, \sqrt{\tau s})}{\int_{\hat{s}_0/s}^1 d\tau \, \mathcal{L}(\tau)}. \quad (24)$$

Figure 2 shows the total multiplicity distribution for Goldstone bosons:

$$\tilde{P}(n, \sqrt{s}) = \sum_{n_z, n_w} \tilde{P}(n_w, n_z, \sqrt{s}) \, \delta_{n \, n_z + n_w} \quad (25)$$

for $\sqrt{s} = 200$ TeV and $\sqrt{\hat{s}_0} = 5$ TeV. Because the luminosity $\mathcal{L}(\tau)$ falls so rapidly, most interactions occur just above the subprocess threshold $\sqrt{\hat{s}_0}$; for our purposes, we could equally well have used $P(n_w, n_z, \sqrt{\hat{s}_0})$

instead of $P(n_w, n_z, \sqrt{\tau s})$ in Eq. (24). In other words, the high-multiplicity tail in Fig. 2 is determined largely by fluctuations in the multiplicity for subprocesses just above threshold and not by fluctuations in the subprocess energy itself.

Turning to the kinematics of multi-w production, we again get inspiration from hadron physics. In analogy with QCD where the bulk of multiparticle production is characterized by limited transverse momentum $\langle p_T \rangle_{\text{QCD}} \simeq 400$ MeV $[= O(\Lambda_{\text{QCD}}) = O(f_\pi)]$ it is natural to assume that multi-w production is similarly governed by a parameter $\langle p_T \rangle_w$. Two plausible $O(v)$ guesses are

$$\langle p_T \rangle_w \simeq M_W, \tag{26}$$

and

$$\langle p_T \rangle_w \simeq \frac{v}{f_\pi} \langle p_T \rangle_{\text{QCD}} \simeq 1 \text{ TeV}. \tag{27}$$

A simple choice for the subprocess cross section $\hat{\sigma}(ww \rightarrow n\, w)$ reflecting limited p_T is given by

$$d\hat{\sigma}(ww \rightarrow n\, w) = F_n(\hat{s}, \hat{s}_0, M_W) \delta^4 \left(P_{\text{total}} - \sum_i p_i \right) \prod_i \frac{d^3 p_i}{2 E_i} \exp\left[-\frac{(p_T^2)_i}{2 \langle p_T \rangle_w^2} \right], \tag{28}$$

where P_{total} is the total four-momentum of the system and p_i are the individual final state momenta. The normalization $F_n(\hat{s}, \hat{s}_0, M_W)$ is chosen so that after integrating over phase space and summing over all possible multiplicities one reproduces the total ww cross section of Eq. (13).

Figures 3 and 4 show the laboratory distributions for gauge boson rapidity y_w and p_T for the case $n = 8$ for a subprocess energy $\sqrt{\hat{s}} = 5$ TeV at $\sqrt{s} = 200$ TeV. A cur-

sory inspection of the p_T distribution for the scale choice $\langle p_T \rangle_w \simeq 1$ TeV confirms what could have been trivially anticipated: that damping transverse momentum beyond $\langle p_T \rangle_w$ is irrelevant if the average subprocess cms energy per particle $\sqrt{\hat{s}}/n \ll \langle p_T \rangle_w$ — for the example at hand $\sqrt{\hat{s}}/n \simeq 625$ GeV is already smaller than $\langle p_T \rangle_w = 1$ TeV so that the eight bodies are effectively distributed according to pure phase space. Consequently, if the p_T scale relevant to strong w dynamics is indeed ~ 1 TeV,
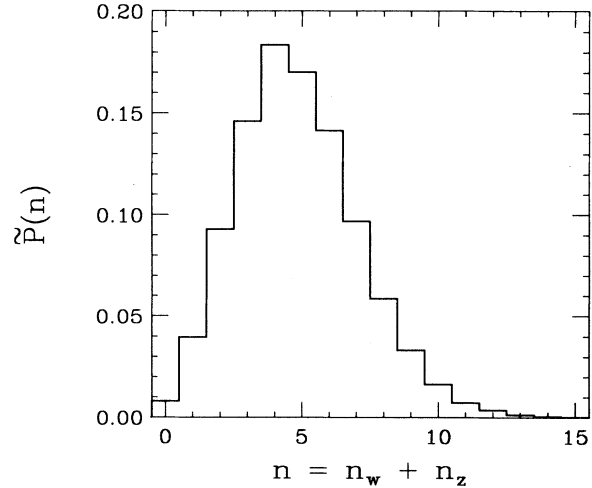

FIG. 2. Goldstone boson multiplicity distribution for $\sqrt{s} = 200$ TeV proton-proton collisions assuming $\sqrt{\hat{s}_0} = 5$ TeV. The distribution is based on charged particle multiplicities measured in $e^+ e^-$ annihilation as described in the text.
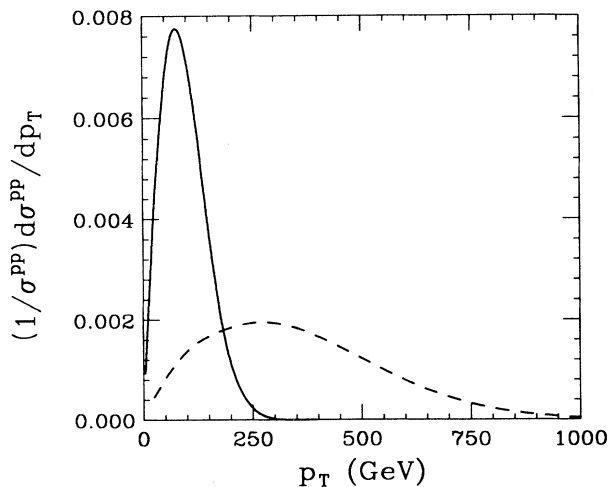

FIG. 3. Transverse momentum distribution for final-state Goldstone bosons for the subprocess $ww \rightarrow 8\, w$ at $\sqrt{s} = 200$ TeV with $\sqrt{\hat{s}_0} = 5$ TeV for p_T scale $\langle p_T \rangle_w = 80$ GeV (solid) and $\langle p_T \rangle_w = 1$ TeV (dashed).
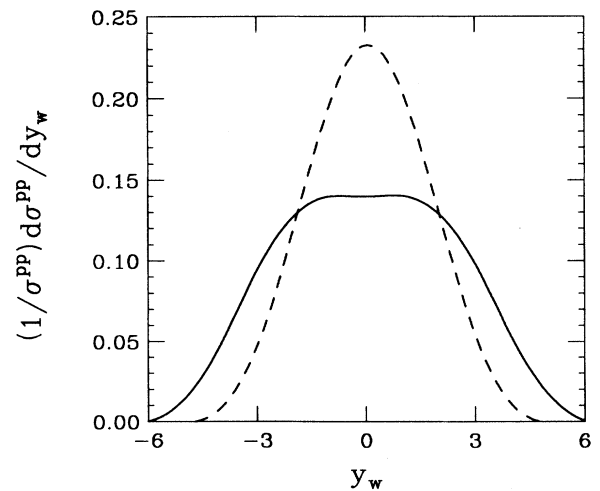

FIG. 4. Laboratory rapidity distribution for final-state Goldstone bosons for the subprocess $ww \rightarrow 8\, w$ at $\sqrt{s} = 200$ TeV with $\sqrt{\hat{s}_0} = 5$ TeV for p_T scale $\langle p_T \rangle_w = 80$ GeV (solid) and $\langle p_T \rangle_w = 1$ TeV (dashed).

multi-w events at $\sqrt{s} = 200$ TeV are essentially spherical and would easily be contained in a laboratory detector. Moreover, the large p_T involved (characterized by the minimum of $\sqrt{\hat{s}}/n$ and $\langle p_T \rangle_w$) gives rise to unambiguous high-p_T leptons and jets, which have no simple standard model background (at least for the production of very many bosons).

The implications of the alternative scale $\langle p_T \rangle_w = M_W$ are less dramatic but deserve closer attention. Though the corresponding laboratory rapidity distribution is certainly broader, even on an event-by-event basis, an overwhelming majority of the Goldstone bosons in the signal still fall within $|y| \leq 3$ relevant to a realistic detector. Of more concern is the p_T distribution since the standard model background production of W bosons or t quarks which subsequently decay to W bosons is also characterized by p_T of $O(M_W)$ or $O(m_t)$. We will return to such backgrounds in the next section.

IV. SIGNATURES AND BACKGROUNDS

The speculative nature of inelastic multi-w production makes the issue of backgrounds difficult to assess in a completely satisfactory manner. Nevertheless, by introducing a few rough, yet plausible, assumptions, we can assess the feasibility of observing a multi-w signal against a background of generic strong and electroweak processes. In this section we decompose the pp multi-w cross section in terms of the experimentally more relevant cross sections for jet plus lepton signatures and compare them to MSM background processes. Since we will only concentrate on rather broad features of the signal and background, we will not attribute overdue significance to our quantitative results; we are only interested in the plausibility of observing inelastic multi-w production.

For definiteness, we will restrict our attention to pp collisions at $\sqrt{s} = 200$ TeV where $\hat{\sigma}_0 = 1$ nb, $\sqrt{\hat{s}_0} = 5$ TeV corresponds to $\sigma^{pp}_{\text{multi-}w} \simeq 190$ fb. Using the n_w, n_z multiplicity distribution of Eq. (24) and the known decay branching fractions for W and Z bosons (see Table I), it is a straightforward exercise to calculate the signal cross section for all possible lepton and jet signatures. It is convenient to characterize signatures by the simultaneous specification of $(n_{Z \to \ell\bar{\ell}}, n_{W \to \ell\nu}, n_{\text{jets}})$, where (1) $n_{Z \to \ell\bar{\ell}}$ is the number of Z decays to e or μ pairs (which we assume are detected and reconstructed with 100% efficiency), (2) $n_{W \to \ell\nu}$ is the number of e or μ presumably arising from leptonic W decays, and (3) n_{jets} is the number of jets presumably arising from the hadronic decays of W and Z bosons. As as simplification, we will assume that all leptons and jets from signal processes (and eventually, all background processes as well) are individually resolved and meet minimum acceptance requirements. In view of the kinematics attributed to multi-w production, we could set minimum acceptance requirements in the neighborhood of $|y| \leq 3$ and $p_T \gtrsim 40$ GeV and be confident that essentially all signal events fall within a realistic detector.

Before we present signal cross sections for various signatures, let us consider possible backgrounds to multi-w production. While the prospect of multiple gauge bosons

TABLE I. Effective decay branching fractions used to estimate the signal and background cross sections for jet plus lepton signatures.

$B(W \to \ell\nu) = 2/9^{\text{a}}$
$B(W \to 2 \text{ jets}) = 7/9^{\text{b}}$
$B(Z \to \ell\bar{\ell}) = 0.067^{\text{a}}$
$B(Z \to \nu\bar{\nu}) = 0.2$
$B(Z \to 2 \text{ jets}) = 0.733$
$B(b \to \ell + 1 \text{ jet}) = 2/9^{\text{a}}$
$B(b \to 1 \text{ jet}) = 7/9$
$B(t \to Wb) = 1$
$B(H \to W^+W^-) = 0.55^{\text{c}}$
$B(H \to ZZ) = 0.26$
$B(H \to t\bar{t}) = 0.19$

[a] Summed over e and μ.

[b] As a simplification, τ decays counted as two-jet decays in this context.

[c] Assumes $m_H = 400$ GeV, $m_t = 140$ GeV, $m_W = 80$ GeV, and $m_Z = 91.17$ GeV.

exploding into existence conjures up images of spectacularly rich multijet plus multilepton signatures, it turns out that at $\sqrt{s} = 200$ TeV such configurations will be commonplace from much less speculative processes. For example, unless one can reliably distinguish between longitudinal and transverse gauge bosons, there will be a large background of multiple W boson events originating from the decays of copiously produced t quarks. In Ref. [20] Barger, Stange, and Phillips have considered the possibility of observing multiple gauge bosons at the LHC and SSC from t quark decay, H boson decay and generic electroweak production processes; their results will provide a convenient starting point for our background estimates.

By minimally extrapolating Fig. 9 of Ref. [20] we obtain the MSM cross sections of Table II (for $m_t = 140$ GeV and $m_H = 400$ GeV) relevant to the direct and indirect (i.e., coming from the decays of t or H) production of multiple gauge bosons at $\sqrt{s} = 200$ TeV. Not all of the cross sections of Table II will be serious backgrounds — most are included so that we can assess their significance relative to $\sigma^{pp}_{\text{multi-}w} \simeq 190$ fb. Furthermore, since we are working on the premise of a strongly coupled Higgs sector (which generally implies a heavy Higgs boson), the cross sections of Table II involving Higgs bosons are most likely overestimates, since they assume a relatively light $m_H = 400$ GeV.

With the exceptions of $\sigma(t\bar{t})$ [which is from an $O(\alpha_s^3)$ calculation] and $\sigma(t\bar{t}b\bar{b})$, none of the processes of Table II include QCD corrections to weak boson production. Additional backgrounds may be obtained by "dressing" each process with QCD radiation. For example, in addition to $t\bar{t}Z$ production, we should also consider the production of $t\bar{t}Zg$, $t\bar{t}Zgg$, etc., corresponding to final states with ad-

ditional hadronic jets. We will return to these additional backgrounds after we consider those of Table II.

Assuming identical acceptance criteria as for the signal, it is a simple combinatoric exercise to convert the cross sections of Table II into background cross sections for various $(n_{Z\to\ell\bar{\ell}}, n_{W\to\ell\nu}, n_{\rm jets})$ signatures. For both our signal and background calculations we used the branching fractions of Table I. The only nontrivial aspect of the background calculation is the treatment of b-quark decays. Since b quarks from t decay retain a non-negligible fraction of the original t quark transverse momentum, $(p_T)_t = O(m_t/2)$, high p_T electrons or muons from leptonic b decays are a background to the leptonic decays of on-shell W bosons. In an idealized decay $b \to \ell + {\rm jet}$, kinematics dictates that the laboratory angular separation of the lepton and jet decreases as the p_T of the parent b quark increases. Following Barger, Stange, and Phillips [20] we assume that we can exploit this small separation and introduce an effective rejection factor of $\simeq 1/40$ for high p_T leptons from b decays. Operationally this means that we suppress cross sections from final states containing n leptons from b decays by a factor of $(1/40)^n$.

Tables III and IV list the signal to background ratios for signatures corresponding to $n_{Z\to\ell\bar{\ell}} = 0, 1$, respectively. The total signal cross section for "gold plated" signatures with two or more leptonically reconstructed Z decays is negligible. For each table entry the quantity in parentheses is the background summed over the

contributing processes of Table II. As mentioned above, additional backgrounds arise if one considers dressing the processes of Table II with QCD radiation. A crude way of accounting for these additional backgrounds is to assume, for example, that $\sigma(t\bar{t}Z + {\rm jet}) \simeq \alpha_s\sigma(t\bar{t}Z)$, $\sigma(t\bar{t}Z + 2\ {\rm jets}) \simeq \alpha_s^2\sigma(t\bar{t}Z)$, etc., where each extra QCD jet costs a factor of α_s (with α_s typically evaluated at the relevant p_T scale of $\simeq 40$ GeV). This simple ansatz is motivated by the results of Behrends et al. [21] who have found, when calculating W plus jets cross sections (including realistic acceptance and isolation criteria), that $R_n = \sigma(W + n\ {\rm jets})/\sigma(W + (n-1)\ {\rm jets}) \simeq 0.2$ at Tevatron energies. Though this procedure certainly has its limitations and has not yet been demonstrated to hold at SSC energies and above (with a corresponding small value of R_n), we will nevertheless adopt it as a rough estimate and use a factor of $(0.2)^n$ to dress cross sections of Table II with n additional QCD jets. The denominator of each entry of Tables III and IV is a sum of the contribution in parentheses and all the relevant "QCD dressed" contributions. For fixed $n_{Z\to\ell\bar{\ell}}, n_{W\to\ell\nu}$, the QCD dressed contribution to the $n_{\rm jets}$ background is equal to $(0.2)^2$ times the total background for $n_{\rm jets} - 2$.

Diagonal entries running from the lower left to upper right of Tables III and IV correspond to signals with a fixed minimum value of $n_w + n_z$. Consider, for example, the entry for $(n_{W\to\ell\nu} = 5, n_{\rm jet} = 8)$ in Table III. As far as the signal is concerned, the five leptons could only have come from five leptonic w decays (remember — we

TABLE II. Standard model backgrounds ($m_t = 140$ GeV, $m_H = 400$ GeV) for multiple gauge boson production at $\sqrt{s} = 200$ TeV obtained by extrapolating the results of Ref. [20] except where noted.

Process	σ (fb)	Process	σ (fb)
$t\bar{t}$	1.1×10^8	$t\bar{t}t\bar{t}$	18 000
$t\bar{t}b\bar{b}$	1.6×10^6	$t\bar{t}H$	8 600
$gg \to H$	2.6×10^5	$t\bar{t}W^+W^-$	3 100
$W^+Z + W^-Z$	2.7×10^5	$t\bar{t}ZZ$	380
W^+W^-	2.4×10^5	$t\bar{t}W^+Z + t\bar{t}W^-Z$	130
ZZ	1.0×10^5	HH	100
$qq \to qqH$	3.1×10^4	$W^+W^-W^+W^-$	50[a]
$qq \to qqW^+W^+$	1.8×10^4	$WWWZ$	22[b]
$qq \to qqW^-W^-$	1.2×10^4	$WWZZ$	10[b]
		$WZZZ$	4[b]
$t\bar{t}Z$	120 000	$ZZZZ$	2[a]
$t\bar{t}W^+ + t\bar{t}W^-$	9 300		
$W^+W^+W^- + W^-W^-W^+$	2 400		
W^+W^-Z	2 000	$HHW^+ + HHW^-$	2[c]
$W^+ZZ + W^-ZZ$	560	HHZ	1[c]
$W^+H + W^-H$	260		
ZH	180		
ZZZ	150	$t\bar{t}t\bar{t}t\bar{t}$	3[d]

[a]Nonresonant contributions taken from Ref. [22].
[b]Estimates obtained by assuming $\sigma(4Z) = f^4\sigma(4W)$ so that each additional Z boson suppresses $\sigma(4W)$ by a factor $f \simeq 0.44$.
[c]Estimates obtained by extrapolating LHC and SSC rates of Ref. [20] assuming a linear relationship between $\ln \sigma$ and $\ln s$.
[d]Estimate obtained by assuming $\sigma(6t)/\sigma(4t) = \sigma(4t)/\sigma(2t)$.

TABLE III. Signal-background cross sections (in fb) at $\sqrt{s} = 200$ TeV for signatures with no leptonic Z decay ($n_{Z \to \ell\bar{\ell}} = 0$). First quantity in denominator is total background; quantity in parentheses is contribution to total from processes of Table II. Cross sections less than 0.005 fb are rounded to zero.

$n_{W \to \ell\nu}$ \ n_{jet}	6	8	10	12	14	16	18
2	$\dfrac{4}{30000(9000)}$	$\dfrac{4}{3000(1000)}$	$\dfrac{3}{200(90)}$	$\dfrac{2}{8(0.8)}$	$\dfrac{1}{0.5(0.2)}$	$\dfrac{0.5}{0.03(0.01)}$	$\dfrac{0.2}{0}$
3	$\dfrac{1}{500(300)}$	$\dfrac{1}{60(40)}$	$\dfrac{0.7}{3(0.9)}$	$\dfrac{0.5}{0.2(0.07)}$	$\dfrac{0.3}{0.02(0.01)}$	$\dfrac{0.1}{0}$	$\dfrac{0.06}{0}$
4	$\dfrac{0.2}{9(7)}$	$\dfrac{0.2}{0.8(0.4)}$	$\dfrac{0.1}{0.05(0.02)}$	$\dfrac{0.09}{0.01(0)}$	$\dfrac{0.05}{0}$	$\dfrac{0.02}{0}$	$\dfrac{0.01}{0}$
5	$\dfrac{0.03}{0.10(0.08)}$	$\dfrac{0.02}{0.01(0)}$	$\dfrac{0.02}{0}$	$\dfrac{0.01}{0}$	$\dfrac{0.01}{0}$	$\dfrac{0}{0}$	$\dfrac{0}{0}$

assume 100% efficiency in identifying and removing Z decays to e or μ pairs). Similarly, the eight jets presumably come from the hadronic decays of four bosons. Thus the visible decay products correspond to a minimum number of nine Goldstone bosons. Only a minimum is determined because there could, in addition, be an arbitrary number of undetected $Z \to \nu\bar{\nu}$ decays. The same conclusion follows by considering any entry along the same diagonal.

Table III, which corresponds to signatures with no leptonically reconstructed Z decays ($n_{Z \to \ell\bar{\ell}} = 0$), indicates that the signal/background (S/B) exceeds unity essentially only for $n_w + n_z \geq 9$. Summing over signatures of Table III, which have $S/B > 1$ gives an overall $S/B = 3.0$ fb/0.8 fb. A detailed decomposition of the background into specific contributions reveals that when the signal emerges from the background (along the diagonal corresponding to $n_w + n_z \geq 9$) the dominant backgrounds are $6t$ production and $4t + $ jets.

Turning to Table IV, which corresponds to signatures containing exactly one leptonically reconstructed Z decay ($n_{Z \to \ell\bar{\ell}} = 1$), we find that $S/B > 1$ for signals with $n_w + n_z \geq 7$. Summing over all signatures of Table IV, which have $S/B > 1$, gives an overall $S/B = 3.6$ fb/0.4 fb. When the signal emerges from the background (along the

diagonal corresponding to $n_w + n_z \geq 7$) the dominant backgrounds are $Ht\bar{t} + $ jets (where $H \to ZZ$) and $Zt\bar{t} + $ jets.

Once again we should emphasize the tentative nature of our numerical results. They are only meant as a rough indication of whether or not inelastic multi-w would be observable at a hadron collider. On the positive side, without exploiting any of the special signal characteristics (e.g., the longitudinal nature of the gauge bosons, large summed transverse energy, the possibility of reconstructing hadronic W and Z decays, etc.) we see that observing inelastic w production is not ruled out (at least for the hypothetical scaled up QCD model we have used). On the other hand, cross sections of ~ 1 fb with $S/B \simeq (1)$ are marginal: a realistic model and a definitive background study could easily introduce cumulative factors of two which could completely alter (for better or worse) the prospects of observing a signal. For example, had we not artificially assumed that all hadronic jets are contained, isolated, and identifiable, then the signal would have been diluted by being spread over signatures with both even and odd numbers of observed jets. With qualifications of this type in mind, our results should only be viewed as a first step towards demonstrating the plausibility of observing inelastic multi-w production.

TABLE IV. Signal-background cross sections (in fb) at $\sqrt{s} = 200$ TeV for signatures with one leptonic Z decay ($n_{Z \to \ell\bar{\ell}} = 1$). First quantity in denominator is total background; quantity in parentheses is contribution to total from processes of Table II. Cross sections less than 0.005 fb are rounded to zero.

$n_{W \to \ell\nu}$ \ n_{jet}	6	8	10	12	14	16	18
1	$\dfrac{1}{200(100)}$	$\dfrac{1}{8(1)}$	$\dfrac{0.9}{0.3(0)}$	$\dfrac{0.6}{0.01(0)}$	$\dfrac{0.3}{0}$	$\dfrac{0.2}{0}$	$\dfrac{0.07}{0}$
2	$\dfrac{0.5}{3(0.9)}$	$\dfrac{0.4}{0.1(0.01)}$	$\dfrac{0.3}{0}$	$\dfrac{0.2}{0}$	$\dfrac{0.1}{0}$	$\dfrac{0.06}{0}$	$\dfrac{0.03}{0}$
3	$\dfrac{0.1}{0.02(0)}$	$\dfrac{0.1}{0}$	$\dfrac{0.08}{0}$	$\dfrac{0.05}{0}$	$\dfrac{0.03}{0}$	$\dfrac{0.02}{0}$	$\dfrac{0.01}{0}$
4	$\dfrac{0.02}{0}$	$\dfrac{0.02}{0}$	$\dfrac{0.02}{0}$	$\dfrac{0.01}{0}$	$\dfrac{0.01}{0}$	$\dfrac{0}{0}$	$\dfrac{0}{0}$

V. SUMMARY AND CONCLUSIONS

Given the number and nature of the assumptions we have made, a brief summary of our whole analysis is in order. After outlining our scaling procedure, we found that a ww total cross section of $\hat{\sigma}_0 = 1$ nb above a ww cms threshold $\sqrt{\hat{s}_0} = 5$ TeV corresponds to a pp cross section of $\simeq 190$ fb at $\sqrt{s} = 200$ TeV. This sets an upper limit on the signal (within the assumptions) — before any kinds of backgrounds, acceptance, efficiencies, etc., are considered.

Going further, we scaled up an assumed hadronic multiplicity distribution and determined how $\sigma^{pp}_{\text{multi-}w} \simeq 190$ fb is partitioned into contributions with fixed multiplicity (see Fig. 2). Because of the rapidly falling ww luminosity, most ww interactions occur just above the assumed threshold $\sqrt{\hat{s}_0}$, which leads to $\langle n_w + n_z \rangle \simeq 4 - 5$. When backgrounds are considered, a naive analysis reveals that signals containing $\lesssim 6$ Goldstone bosons are likely dominated by generic backgrounds and suggests that the potentially detectable signal resides largely in the high-multiplicity tail of the multiplicity distribution. This restriction reduces the original 190 fb approximately by a factor of 2.

Signatures roughly consisting of (a) at least two high p_T leptons (presumably from W decay) and ten or more jets or (b) one leptonically reconstructed Z, one or more high p_T leptons and eight or more jets have a combined cross section of a few fb, which is a factor of 4–5 above the background. Of course, given the nature of the assumptions involved, these cross sections are not to be taken literally — they are only meant to be indicative of the strengths or weaknesses of a multi-w signal. A relatively interesting conclusion, however, is that if strong multi-w production is to be observed over conventional backgrounds, the inelastic production of three or four longitudinal bosons is likely not sufficient; one has to consider the productions of seven or more bosons. The

frequency of such high-multiplicity states will likely depend critically upon the details of the underlying strongly interacting theory.

If one is willing to entertain the notion of inelastic ww physics above a ww cms threshold as low as $\sqrt{\hat{s}_0} = 1$ TeV, then most of our results still hold and are of relevance to the SSC physics program. As can be deduced from Fig. 2, the total signal rates for $(\sqrt{s} = 200 \text{ TeV}, \sqrt{\hat{s}_0} = 5$ TeV) are identical to those for $(\sqrt{s} = 40 \text{ TeV}, \sqrt{\hat{s}_0} = 1$ TeV). Since the average charge multiplicity $\langle n_w \rangle$ is a slowly varying function of $\sqrt{\hat{s}}$ a reduced threshold does not change the overall w and z multiplicity significantly. On the other hand, all the background rates at the SSC are lower than at $\sqrt{s} = 200$ TeV.

The broad conclusion to be drawn is that it appears feasible to observe multi-w production arising from a strongly interacting Higgs sector (if such a sector exists at all). Since the energy scale at which inelasticity sets in is generally determined by the masses of the low-lying resonances of the underlying strongly interacting theory, our results are only suggestive (since they arise from conservatively assuming a rather high threshold of 5 TeV). Nevertheless, our results are rather encouraging and suggest that the inelastic W_L and Z_L production may provide an interesting window to the mechanism of strongly broken electroweak symmetry.

ACKNOWLEDGMENTS

[1] E. Farhi and L. Susskind, Phys. Rep. **74**, 277 (1981).

[2] J.M. Cornwall, D.N. Levin, and G. Tiktopoulos, Phys. Rev. D **10**, 1145 (1974); **11**, 972(E) (1975).

[3] M.S. Chanowitz and M.K. Gaillard, Nucl. Phys. **B261**, 379 (1985).

[4] For recent summaries see, e.g., M.S. Chanowitz, in *Perspectives on Higgs Physics*, edited by G. Kane (World Scientific, Singapore, in press); J.A. Bagger, in *Proceedings of the XXVIth International Conference on High Energy Physics*, Dallas, Texas, 1992, edited by J. Sanford (AIP, New York, 1993).

[5] M. Chanowitz and M.K. Gaillard, Phys. Lett. **142B**, 85 (1984).

[6] R.S. Chivukula and M. Golden, Phys. Lett. B **267**, 233 (1991); S.G. Naculich and C.-P. Yuan, *ibid.* **293**, 395 (1992); **293**, 405 (1992).

[7] B.W. Lee, C. Quigg, and H.B. Thacker, Phys. Rev. D **16**, 1519 (1977).

[8] M. Gell-Mann and M. Levy, Nuovo Cimiento **16**, 705 (1960).

[9] S. Weinberg, Phys. Rev. Lett. **17**, 616 (1966).

[10] M.S. Chanowitz, Annu. Rev. Nucl. Part. Sci. **38**, 323 (1988); M.S. Chanowitz and M. Golden, Phys. Rev. Lett. **61**, 1053 (1988); **63**, 466(E) (1989); A. Dobado and M.J. Herrero, Phys. Lett. B **228**, 195 (1989); J.F. Donoghue and C. Ramirez, *ibid.* **234**, 361 (1990); A. Dobado, M.J. Herrero, and T.N. Truong, *ibid.* **235**, 129 (1990).

[11] For a proposed analogy between QCD and the high-energy behavior of the weak *gauge* sector (as opposed to the weak symmetry-breaking sector which we consider) see, e.g., A. Ringwald and C. Wetterich, Nucl. Phys. **B353**, 303 (1991); A. Ringwald, F. Schrempp, and C. Wetterich, *ibid.* **B365**, 3 (1991).

[12] G. 't Hooft, in *Recent Developments In Gauge Theories*, Proceedings of the Cargese Summer Institute, Cargese, France, 1979, edited by G. 't Hooft *et al.*, NATO Advanced Study Institute Series B: Physics Vol. 59 (Plenum, New York, 1980); E. Witten, Nucl. Phys. **B160**, 57 (1979).

[13] R.S. Chivukula, M.J. Dugan, and M. Golden, Phys. Rev. D **47**, 2930 (1993).

[14] Particle Data Group, K. Hikasa *et al.*, Phys. Rev. D **45**,

S1 (1992).

[15] See, e.g., J.J.J. Kokkedee, *The Quark Model* (Benjamin, New York, 1969).

[16] M. Derrick *et al.*, Phys. Rev. D **34**, 3304 (1986).

[17] P. Abreu *et al.*, Z. Phys. C **50**, 185 (1991).

[18] G.L. Kane, W.W. Repko, and W.B. Rolnick, Phys. Lett. **148B**, 367 (1984); S. Dawson, Nucl. Phys. **B249**, 42 (1985).

[19] J.G. Morfin and W.-K. Tung, Z. Phys. C **52**, 13 (1991).

[20] V. Barger, A.L. Stange, and R.J.N. Phillips, Phys. Rev. D **45**, 1484 (1992).

[21] F.A. Behrends, H. Kujif, B. Tausk, and W.T. Giele, Nucl. Phys. **B357**, 32 (1991).

[22] V. Barger, T. Han, and H. Pi, Phys. Rev. D **41**, 824 (1990).